

2014

# Performance Measurement of Revolving Vane Compressor

Kok Ming Tan

SANDEN INTERNATIONAL SINGAPORE PTE LTD, SINGAPORE, tan\_kok\_ming@sanden.com.sg

Wei Chong Choo

SANDEN INTERNATIONAL SINGAPORE PTE LTD, SINGAPORE, choo\_wei\_chong@sanden.com.sg

Michael Chee

SANDEN INTERNATIONAL SINGAPORE PTE LTD, SINGAPORE, michael\_chee@sanden.com.sg

Ken Law

SANDEN INTERNATIONAL SINGAPORE PTE LTD, SINGAPORE, ken\_law@sanden.com.sg

Ismail Iswan

SANDEN INTERNATIONAL SINGAPORE PTE LTD, SINGAPORE, ismail\_iswan@sanden.com.sg

*See next page for additional authors*

Follow this and additional works at: <https://docs.lib.purdue.edu/icec>

---

Tan, Kok Ming; Choo, Wei Chong; Chee, Michael; Law, Ken; Iswan, Ismail; and Ooi, Kim Tiow, "Performance Measurement of Revolving Vane Compressor" (2014). *International Compressor Engineering Conference*. Paper 2301.  
<https://docs.lib.purdue.edu/icec/2301>

This document has been made available through Purdue e-Pubs, a service of the Purdue University Libraries. Please contact [epubs@purdue.edu](mailto:epubs@purdue.edu) for additional information.

Complete proceedings may be acquired in print and on CD-ROM directly from the Ray W. Herrick Laboratories at <https://engineering.purdue.edu/Herrick/Events/orderlit.html>

---

**Authors**

Kok Ming Tan, Wei Chong Choo, Michael Chee, Ken Law, Ismail Iswan, and Kim Tiow Ooi

## Performance Measurement of Revolving Vane Compressor

Kok Ming TAN<sup>1\*</sup>, Wei Chong CHOO<sup>1</sup>, Michael CHEE<sup>1</sup>, Ken LAW<sup>1</sup>, Ismail ISWAN<sup>1</sup>, Kim Tiow OOI<sup>2</sup>

<sup>1</sup>Sanden International Singapore Pte Ltd,  
Sanden House, 25 Ang Mo Kio Street 65, Singapore 569062  
Phone: +65 63113059 E-mail: tan\_kok\_ming@sanden.com.sg

<sup>2</sup>School of Mechanical & Aerospace Engineering,  
Nanyang Technological University, Nanyang Avenue, Singapore 639798  
Phone: +65 67905511 E-mail: mktooi@ntu.edu.sg

\* Corresponding Author

### ABSTRACT

This paper shows and discusses the development of a novel compressor design, Revolving Vane compressor. Firstly, the concept of the novel compressor mechanism and its prototype design will be presented. Secondly, the performance measurements of the first Revolving Vane compressor prototype will be discussed and the mathematical model validations will also be shown. The measurements show that the preliminary compressor prototype exhibits a reliable functional refrigerant-type compressor mechanism. The compactness of the design and the simplicity in the construction enable the Revolving Vane compressor to be great potential for applications in various heating and cooling systems.

### 1. INTRODUCTION

Over the years, rotary compressors have gained popularity and widely used in household and automotive air-conditioning applications because of the compact nature and silent characteristics. By engaging a revolutionary concept to elevate the rotary compressor efficiency, a novel compressor mechanism, named the Revolving Vane (RV) compressor is invented (Teh and Ooi, 2006).

A prototype R134a RV compressor was designed, fabricated, instrumented and tested. The volumetric displacement is 60 cc. Tests were conducted at constant speed under variations suction and discharge pressures and, different oil circulation ratios. For each of the tests, refrigerant mass flow rate, power consumption, suction and discharge temperatures and pressures were recorded. Mathematical models have also been formulated and the measurement was used to validate the models.

### 2. REVOLVING VANE COMPRESSOR

#### 2.1 Revolving Vane Compressor Concept

The configuration of an RV compressor is shown in Figure 1. There are four basic components and these are an outer cylinder, an inner rotor, a sliding vane and a pair of swiveling shoe (Tan and Ooi, 2011). The centers of the cylinder and the rotor are at a distance to form the common line of tangent along the inner and outer circumferences of the cylinder and the rotor and hence, a crescent-shaped working volume is formed. The vane is rigidly fixed to the rotating cylinder at one end and is disposed inside the vane slot of the rotor, at the other end. The vane is in sliding engagement with a pair of swiveling shoe and divides the crescent-shaped volume into two individual chambers.

During the operation, the cylinder rotates the rotor through the fixed vane. Both rotor and cylinder rotate at their respective own rotational axes. Hence, the volumes on either sides of the vane increases and decreases simultaneously, resulting in suction, compression and discharge of the working fluid.

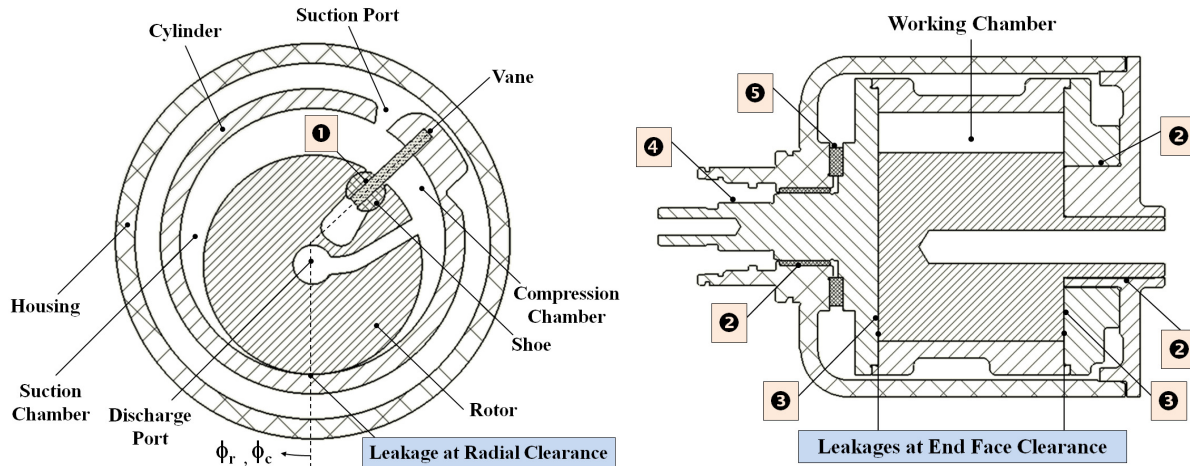


Figure 1: First Prototype of Revolving Vane Compressor

## 2.2 Prototype Design

The first prototype of RV compressor is designed with a volumetric displacement of 60 cc. With reference to Figure 1, the suction gas passes through the suction port on the circumferential surface of the cylinder before it flows into the suction chamber. The gas within the compression chamber will be discharged through the passage located at the center of the rotor. The discharge gas flows through an in-built oil separator where the lubricant will be forced to be left behind and flows into the oil sump while the refrigerant gas is being discharged. During the operation, both the rotating cylinder and rotor are each supported by a set of plain journal bearings.

The prototype design is guided closely by an in-house computer model. The model addresses the thermodynamics aspects of the working fluid in the compressor working chamber during operation namely the variations of the instantaneous pressure, temperature and mass. The established pressure profile is then used together with the computed inertial and frictional forces to evaluate the resultant forces acting on each of the components such that the dimensions of the plain bearing can be determined. Prior to this, the oil film thickness for the plain journal bearing will be computed to assess the feasibility of the surface roughness of the lubricated surfaces of the bearings. As a result, the critical design dimensions are set and the corresponding predicted performance can be assessed.

The frictional losses and the main leakage area in RV compressor are shown in Figure 1. The frictional losses associated with the compressor can be predicted by Equations (1) to (5).

### ❶ Vane Side Frictional Loss (Tan and Ooi, 2011)

$$P_{vs} = \eta_{vs} \times \frac{I_r \times \alpha_r}{R_r \cos(\phi_r - \phi_c)} \times V_v \quad (1)$$

### ❷ Oil-Film Type Bearing Frictional Loss (Hirani et al., 1999)

$$P_{f,Br} = R_{Br} \times \omega_j \times \left[ \frac{\mu \omega_j R_{Br}^2 L_{Br} \pi}{\delta_{Br} \sqrt{1-\epsilon^2}} \left( \frac{2+\epsilon}{1+\epsilon} \right) + \frac{\delta_{Br} \epsilon}{2R_{Br}} \sqrt{F_x^2 + F_y^2} \sin \Phi \right] \quad (2)$$

### ❸ End Face Frictional Loss (Subiantoro and Ooi, 2011)

$$P_{ef} = \frac{\mu}{\delta_{ef}} \pi \left[ \omega_c^2 e^2 R_r^2 + \frac{1}{2} (\omega_c - \omega_r)^2 R_r^4 \right] + \frac{\mu}{\delta_{ef}} \pi \left[ e^2 (\omega_c^2 R_r^2 - \omega_r^2 R_{cc}^2) + \frac{1}{2} (\omega_c - \omega_r)^2 (R_r^4 - R_{cc}^4) \right] \quad (3)$$

④ Lip Seal Frictional Loss (Muller and Nau, 1998 )

$$P_{f,ls} = 2\pi\psi R_s^2 \omega_s \quad (4)$$

⑤ Thrust Bearing Frictional Loss

$$P_{th,Br} = \pi\mu\omega_s P \frac{(d_o^3 - d_i^3)}{12} \quad (5)$$

The sum of the above frictional losses and the indicated power defines the compressor power consumption. On the other hand, the internal leakage caused by pressure difference of the connecting chambers is estimated by an orifice flow model.

### 3. SETUP OF EXPERIMENT

#### 3.1 Inspection of Geometrical Properties

The geometrical dimensions of every compressor components were carefully examined as this determines the success or otherwise the entire compressor unit. For example, the diameters of the shaft and the bearing dictate the bearing clearance in which the oil film is able to operate within full film lubrication conditions. Besides, the surface finish of the shaft-bearing pair was also checked. The existence of sharp peaks in the surface roughness profile should be carefully examined as these peaks would jeopardize the bearing performance or to the worst, bearing seizure may occur during operation. The surface roughness of the rotating cylinder shaft and its bearing are shown in Figure 2. The root mean square surface roughness value for the rotating cylinder shaft and its bearing are  $0.3 \mu\text{m}$  and  $0.4 \mu\text{m}$ .

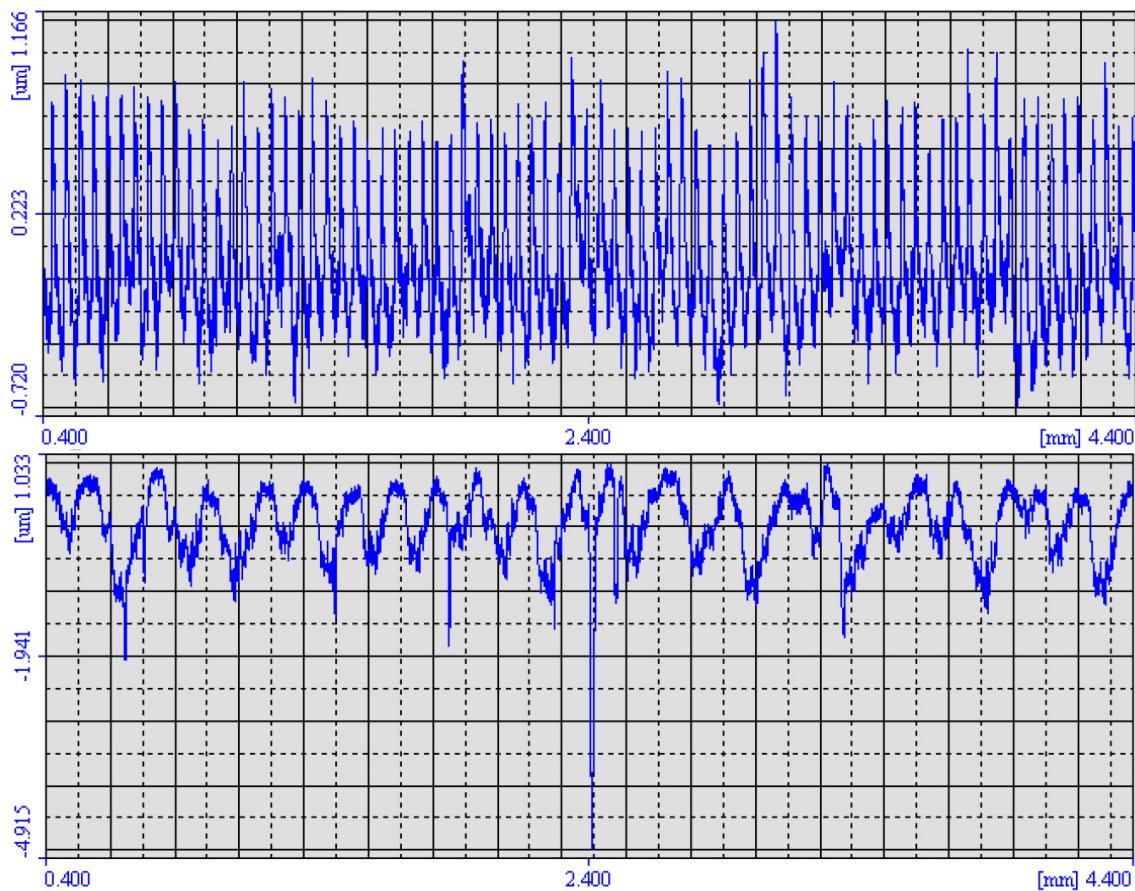


**Figure 2:** Surface Roughness Profile of Cylinder Shaft (Upper Graph) and its Bearing (Lower Graph)

### 3.2 Inspection of Part Balancing

The mass properties of the rotating assemblies are important because if these are improperly balanced, unwanted centrifugal forces will be incurred and cyclic loading on the bearing will occur, which in turn affects the bearing performance characteristics, or may lead to compressor failure.

During the design phase, the rotating assemblies are theoretically balanced under the static and dynamic modes. Both rotating assemblies were inspected using balancing machines as shown in Figure 3, to ensure the validity of the theoretical approach. The amount of imbalance force due to the effects of the non-uniform material density distribution and allowable tolerance during assembly process for both rotor and cylinder assemblies at speed of 2000 rev/min are 7.2 N and 2.9 N respectively. The unbalance forces are insignificant to the active forces which are of the order of kN.

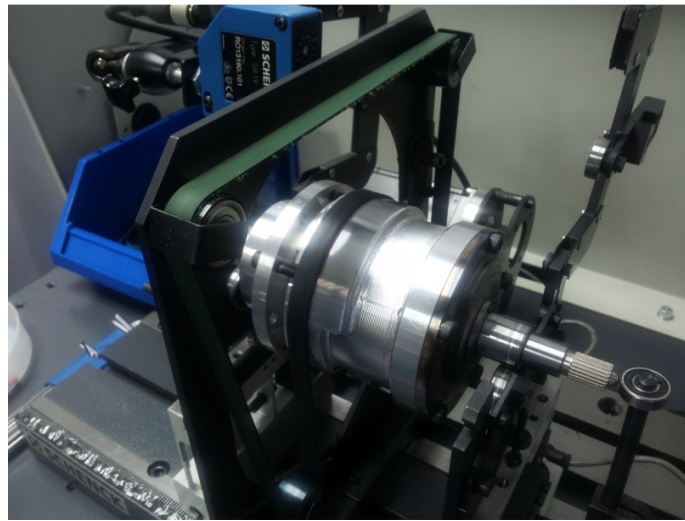


**Figure 3:** Cylinder Sub-Assembly under Balancing Examination

## 4. PERFORMANCE MEASUREMENT & MATHEMATICAL MODELS VALIDATION

### 4.1 Performance Measurement

Figure 4 shows the RV compressor prototype in a calorimeter. R134a was used as the working fluid and the compressor is belt driven to operate at a constant speed of 2000 rev/min throughout the entire test. The compressor prototype is tested under variations of suction and discharge pressures and with different oil circulation ratios (OCR). The measured parameters are mass flow rate and power consumption. The test is divided into 3 phases and the details of which are shown in Table 1. The type of compressor built refers to the type of approach during assembly process. The random and controlled assembly process results in different radial clearance distribution during one complete compressor revolution. The superheat is the measured temperature difference of the refrigerant gas in between saturation condition and evaporator outlet under the constant evaporating pressure.

**Table 1:** Revolving Vane Compressor Test Plan

	1 <sup>st</sup> Measurement	2 <sup>nd</sup> Measurement	3 <sup>rd</sup> Measurement
Objective	To compare the effect of radial clearance	To compare the effect of radial clearance	To examine the effect of OCR
Type of Compressor Built	Random	Controlled	Controlled
Superheat (°C)	5	5	10
OCR	2.5 %	2.5 %	2.5 % to 10 %

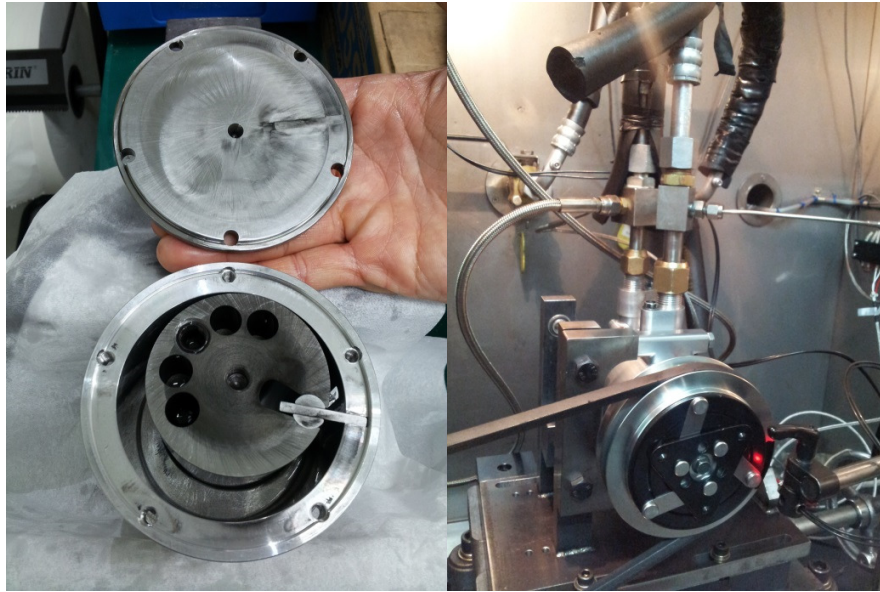


**Figure 4:** Revolving Vane Compressor and its Prototype in Calorimeter

Figure 5 shows the results of the first functional test for revolving vane compressor. The ratios of mass flow rate with respect to that at minimum pressure ratio of 3.12 are shown in the figure. The first measurement phase achieves a pressure ratio of 3.62. The mass flow rate drops by 22% as the pressure ratio increases from 3.12 to 3.62. It is known that the magnitude of radial clearance is critical in affecting the internal leakage which directly affects the effective mass flow rate. Therefore, relentless effort has been spent to discover and define the relationship between all participating geometrical dimensions and tolerance factors in order to manipulate the radial clearance distribution throughout one complete revolution. As a result, during second measurement phase, the radial clearance towards the compression end has been manipulated to be tighter by  $10\ \mu\text{m}$  and the resultant mass flow rate has been improved by 16% and 27% at pressure ratio of 3.12 and 3.37 respectively. It is observed that higher pressure ratio of 5.32 can be achieved with properly assembled radial clearance.

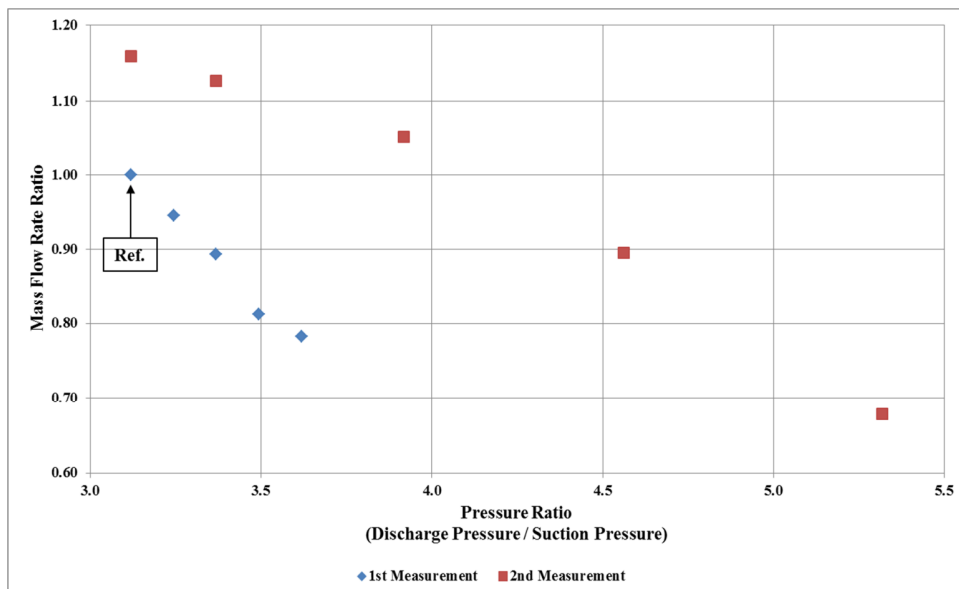


**Figure 5:** Measured Mass Flow Rate Ratio

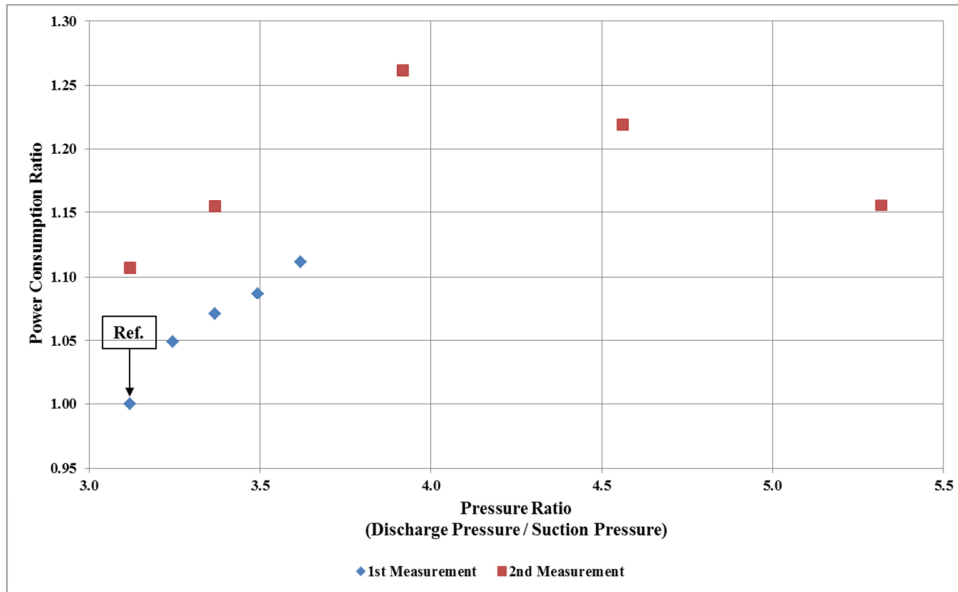


**Figure 6:** Measured Power Consumption Ratio

The power consumption of the compressor has also been measured and its ratios with respect to that at the minimum pressure ratio of 3.12 are shown in Figure 6. The low power consumption of the compressor during the first measurement is due to the larger radial clearance. The know-how on getting a better radial clearance applied during second measurement phase and thus improves effective mass flow rate as well as increases the power consumption. The power consumption has been increased by 10.7 % and 7.8 % at pressure ratio of 3.12 and 3.37 respectively.

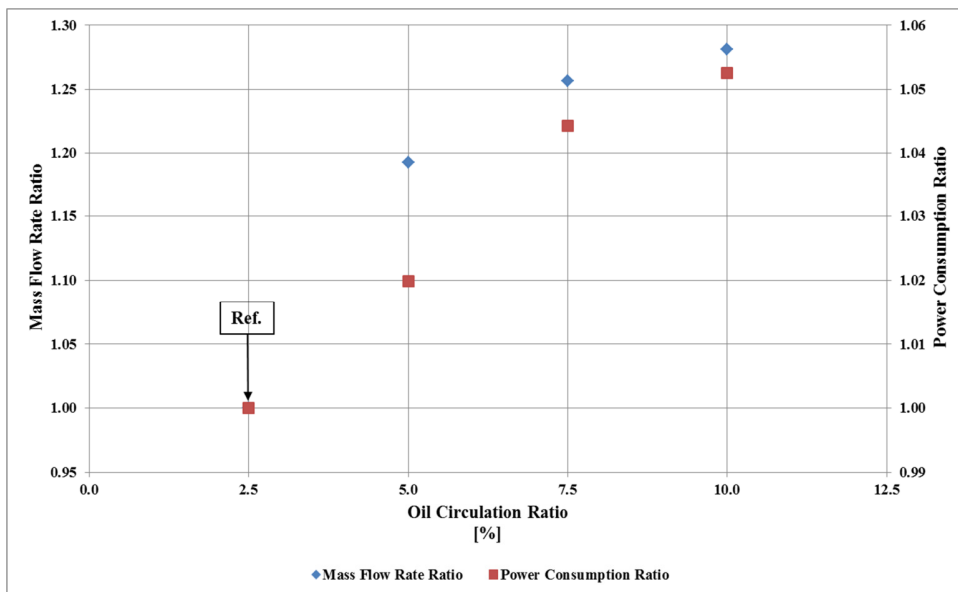


**Figure 7:** Effects of Oil Circulation Ratio (OCR)

The third measurement examined the effect of oil circulation ratio (OCR) and the results are shown in Figure 7. The measurement for OCR at 2.5% is set as a reference. At a pressure ratio of 5.32, the mass flow rate increases by 28% when OCR increases from 2.5% to 10%. This is because the internal sealing by oil is improved by having more oil circulation ratio. It is logical that power consumption increases accordingly as the mass flow rate increases. The power consumption increases by 5.3 % when OCR increases by 7.5 % at pressure ratio of 5.32.



#### 4.2 Mathematical Models Validation

The comparisons between the measured and the predicted mass flow rate and power consumption of the 2<sup>nd</sup> measurement are expressed in a ratio form and shown in Figure 8. The error bars are obtained by using the RSS method of uncertainty analysis and it is generally at 3% in the case of power consumption measurement. The ratio between measured and predicted power consumption shown in Figure 8 shows good agreement, with a maximum discrepancy of 11.8 % at pressure ratio of 3.12. The discrepancy is expected to decrease if the local lubricating oil viscosity at the bearings can be obtained. The local lubricating oil viscosity at the bearing can be predicted by considering thermal energy balance network to the entire compressor to account for the effects of heat transfer among compressor components, oil and refrigerant flow under the operating conditions.

The ratio between measured and predicted mass flow rate is shown in the same figure. It is observed that the maximum discrepancy of 7.4% at pressure ratio of 3.12 is shown. The comparison shows the predicted flow rate is always less than the measured flow rate. This is because the effect of oil sealing due to existence of oil film thickness along leakage path is not taken into consideration in mass flow rate prediction. The prediction accuracy can be further improved by considering the effect of oil-refrigerant mixing.

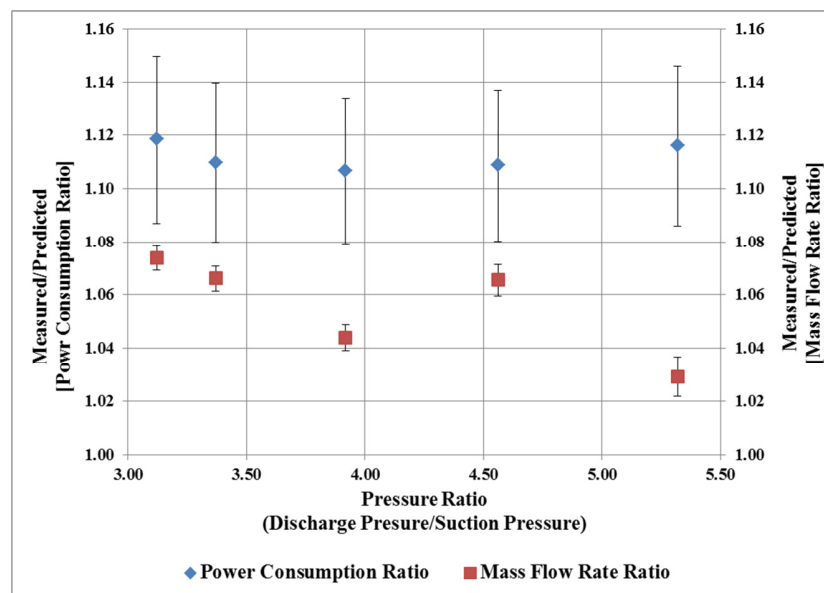


**Figure 8:** Comparisons of Measurement to Prediction

### 5. CONCLUSIONS

In this paper, the prototype machine for Revolving Vane compressor has been designed, tested and its preliminary performance has been measured. The following has been obtained:

- 1) The revolving vane mechanism has been proven to function reliably in a refrigeration compressor. The prototype has operated at speed of 2000 rev/min using R134a as working fluid and attained pressure ratio of 5.32. In addition, more than 30 hours of operation have been clocked.
- 2) The importance of the variations of radial clearance throughout one complete revolution and the amount of lubricant circulation rate are highlighted in the performance measurement. The know-how on in getting the required assembled radial clearance has been grasped.
- 3) The mathematical model accounting for frictional and leakage losses have been validated through the measurements. Good agreement has been obtained between predicted and measured results. The maximum discrepancies for power consumption and mass flow rate are 11.8% and 7.4% respectively.

The preliminary assessments have provided a great confidence in the functionality of the novel Revolving Vane compressor design. The simple geometry makes it easy to manufacture and ease of precision. It is believed that the Revolving Vane compressor is capable to compete commercially with other existing state of the art and well suited for cooling and heating applications.

### NOMENCLATURE

d	diameter	(m)
e	eccentricity	(m)
F	force	(N)
I	rotational inertia	(kg m <sup>2</sup> )
L	length	(m)
P	power	(W)
R	radius	(m)
V	velocity	(m s <sup>-1</sup> )
$\alpha$	angular acceleration	(rad s <sup>-2</sup> )
$\delta$	clearance	(m)
$\varepsilon$	eccentricity ratio	(-)
$\eta$	friction coefficient	(-)
$\psi$	force per unit length	(N m <sup>-1</sup> )
$\phi$	angular position	(rad)
$\Phi$	bearing attitude angle	(rad)
$\mu$	viscosity	(Pa s)
$\omega$	angular velocity	(rad s <sup>-1</sup> )

### Subscript

Br	bearing
c	cylinder
cc	cylinder cover
ef	end face
f	friction
i	inner
J	journal
ls	lip seal
o	outer
r	rotor
s	shaft
th	thrust
v	vane
vs	vane side
x	x-direction
y	y-direction

### REFERENCES

- Hirani, H., K. Athre, et al., 1999, Dynamically loaded finite length journal bearings: analytical method of solution, *Journal of Tribology* Vol.121: p. 844-852
- Müller, H. K. and B. S. Nau, 1998, *Fluid Sealing Technology: Principles and Applications*
- Subiantoro, A. and K. T. Ooi, 2011, Analytical Study of the Endface Friction of the Revolving Vane Mechanism, *International Journal of Refrigeration* Vol.34, No.5: p. 1276-1285

Tan K.M. and Ooi K.T., 2011, A Novel Revolving Vane Compressor with a Fixed-vane, International Journal of Refrigeration, Vol.34, No.8: p.1980-1988

Teh Y.L and Ooi K.T, 2006, Design and Friction Analysis of the Revolving Vane Compressor, Proc. Purdue Compressor Technology Conference, C046